# Comparison of Hybrid III head response to shock tube and explosive blast loading

Samuel Maach, Bert von Rosen, Lorne McCauley, Jeffrey Levine, Jean-Philippe Dionne

***Abstract*** Full-scale explosive blast testing is too involved for routine testing of blast protective helmets. In contrast, gas-driven shock tubes are cost-effective, do not require high explosives and generate repeatable shock waves, making them, at first glance, appealing for routine helmet testing. However, previous studies have demonstrated that the flow field outside a shock tube does not represent that which is generated in a free-field blast test. The objective of this paper is thus to demonstrate how this flow field difference affects headform response, given that standard methods for helmet impact attenuation involve surrogate headforms and corresponding acceleration measurements. To that end, a headform instrumented with linear accelerometers was subjected to both shock tube (headform outside the tube) and free-field explosive loading. The explosive charge and standoff distance for full-scale explosive blast testing were selected to replicate static blast parameters previously set for the shock tube testing. Preliminary findings indicate that matching peak static pressure and peak impulse with a headform outside a shock tube does not appropriately reproduce free-field explosive blast headform inertial responses in terms of acceleration, velocity and excursion time histories.

***Keywords*** Blast waves, Explosive testing, Headform, Shock tube, Head Kinematics

## I. INTRODUCTION

Gravity-driven drop towers have long been mandated by standard methods for physical testing of helmets intended to be worn during recreational/sports, professional or transportation activities [1-2]. Test protocols consist of dropping an instrumented headform fitted with the subject helmet and measuring the resulting deceleration when the helmet strikes a rigid anvil. The peak deceleration value is then used as an indication of the impact protection afforded by the subject helmet. Drop tower test protocols are simple, cost-effective and generate repeatable data, which makes them suitable for routine laboratory helmets evaluation during either product development or performance rating according to specific standards [3], despite the fact that no injury predictions can be made directly from these tests.

Similarly, shock tubes have the potential to address laboratory needs for quick and affordable testing of the blast attenuation performance of helmets. Unlike the drop tower case however, there exists no publicly available standard protocol for shock tube testing due to the inherent complexity of blast loading, as compared to blunt impact.

Previous shock tube helmet evaluations compared the pressure histories around the perimeter of military helmets mounted on a 50th percentile male Hybrid III mannequin head subjected to free-field blast waves either inside a conical shock tube [4] or outside a cylindrical shock tube [5]. While experiments whereby the headform and helmet were placed inside a conical shock tube were found to reasonably replicate free-field environments, experiments with the headform and helmet located in the exit jet of a cylindrical shock tube demonstrated significant deviations from free-field blast [6]. These studies did not, however, report any data on the inertial response of the headform itself (linear or angular accelerations), which are the metrics of choice when evaluating or comparing the effectiveness of helmets.

To address this gap, the present study directly compares the dynamic responses of the same headform to equivalent (similar static overpressure and blast impulse) shock tube and free-field explosive blast loading. This preliminary study focuses on unprotected headforms to provide baseline data towards eventual blast attenuation performance evaluations of helmets.

S. Maach (e-mail: samuel.maach@canada.ca; tel: +1-613-947-7534) is Director, B. von Rosen is a Senior Researcher and L. McCauley is a Senior Technologist, all at the Canadian Explosives Research Laboratory (CanmetCERL), Natural Resources Canada. J. Levine is a Research Engineer and J. P. Dionne is Director of Research Engineering at Med-Eng, Ottawa, Canada.

## II. METHODS

### *Head Surrogate*

Similar to previous studies relying on shock tubes to reproduce shock waves [7] and those using free-field blast [8] to evaluate helmets, an instrumented and pre-calibrated 50th percentile male Hybrid III mannequin head and neck assembly (Humanetics, Denton, OH) was used in this study (Fig. 1).

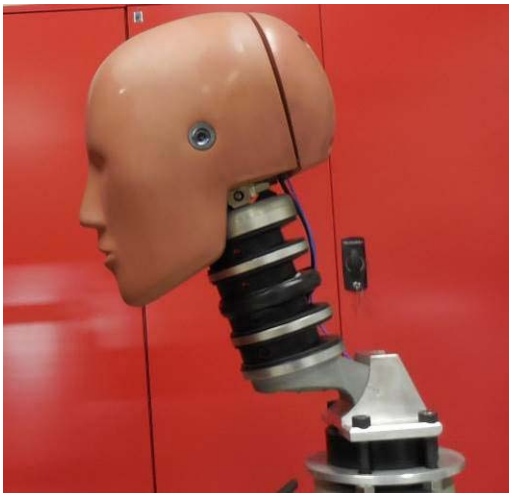

Fig. 1. Hybrid III head and neck assembly used for the shock tube and free-field explosive trials.

### *Shock Tube Configuration*

The Hybrid III head and neck assembly was subjected to blast loading from a 0.30 m diameter shock tube, with a 0.22 m long driver section and a 3.2 m driven section (Cadex, St-Jean-sur-Richelieu, Québec, Canada). Mylar sheets (Dupont Tejjin Films, Chester, VA) were used as rupture diaphragms to burst in such a way as to generate waves near the tube exit that approximate idealised free-field blast waves. The shock tube was open-ended, with the Hybrid III head and neck assembly secured 0.15 m away from the muzzle, measured from the base of the nose (Fig. 2 and Fig. 3). The neck orientation has been set at its standard 0° position.

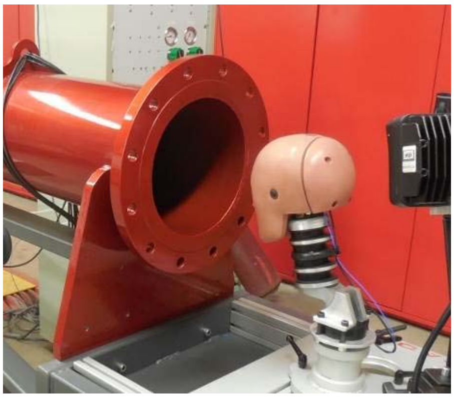

Fig. 2. Open-ended shock tube used at CERL for these tests.

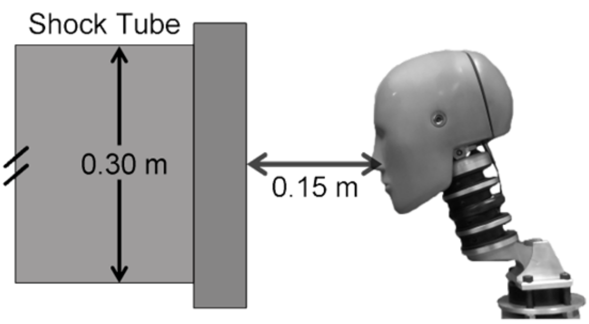


Fig. 3. Location of the Hybrid III headform relative to the shock tube end.

### *Free-Field Blast Test Configuration*

Free-field blast explosive testing was conducted outdoors, on a concrete pad (Fig. 4). A hemispherical charge of C4 high explosive was placed on a 0.075 m x 0.075 m x 0.013 m-thick piece of high-density polystyrene, which was placed on a 0.3 m x 0.3 m x 0.013 m-thick piece of steel. The steel was placed on the ground (concrete pad). A Diped high-strength detonator was inserted through the top of the charge into its centre. The base of the Hybrid III neck was bolted to the edge of a 296 kg steel pad (1.22 m x 2.44 m x 0.013 m) laid on a concrete floor.

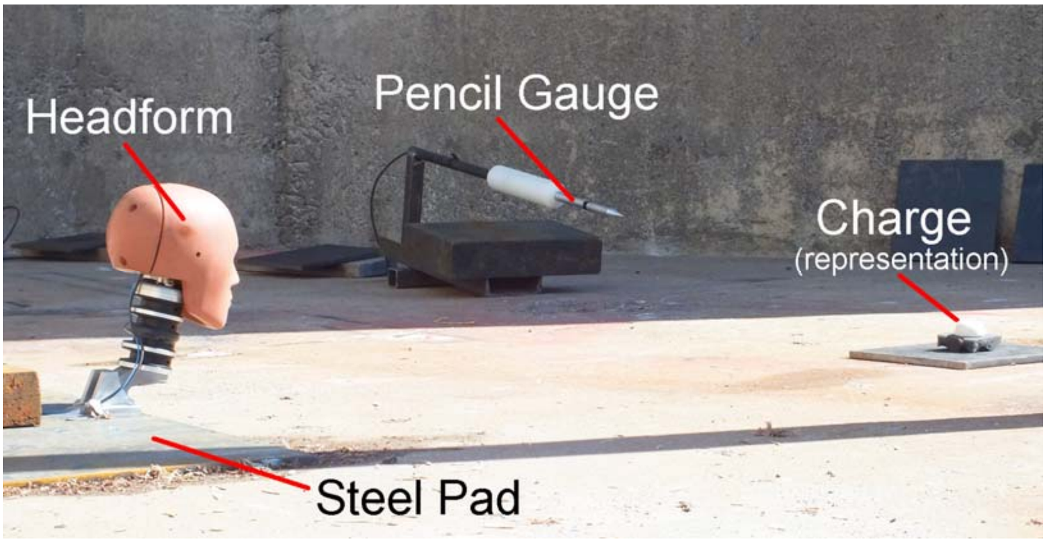


Fig. 4. Hybrid III head and neck assembly subjected to outdoors blast testing.

***Instrumentation***

A set of orthogonal linear accelerometers (PCB model 350B50 triaxial accelerometer, PCB, Depew, NY) was placed inside the headform as shown in Fig. 5. Reference piezo-electric static overpressure sensors (PCB 137A23, Depew, NY) held in a pencil gauge were also used to capture the static overpressure wave details, for both the shock tube (prior to the tests with the headform) and free-field (simultaneously with the headform test) configurations.

The PCB sensor data (pressure and acceleration) was acquired at a rate of 100 kHz using a Yokogawa (SL1000, Newnan, GA) data acquisition system. The mannequin data was filtered according to the established SAE-J211 standard [9]. Specifically, the head acceleration data was processed with a CFC 1000 filter. The pressure data was not filtered. All collected traces were zeroed based on the first 100 data points, and the data was collected for 150 ms in the shock tube tests (including 5 ms of pre-trigger), and 300 ms in the free-field blast tests (including 30 ms of pre-trigger).

In parallel, a high-speed camera (NAC GX-8, Japan) recorded the head excursion in both set-ups (Fig. 6) at a rate of 2,500 frames per second. The head displacement was tracked and analysed using the ProAnalyst tracking system package (XCitex, Woburn, MA).

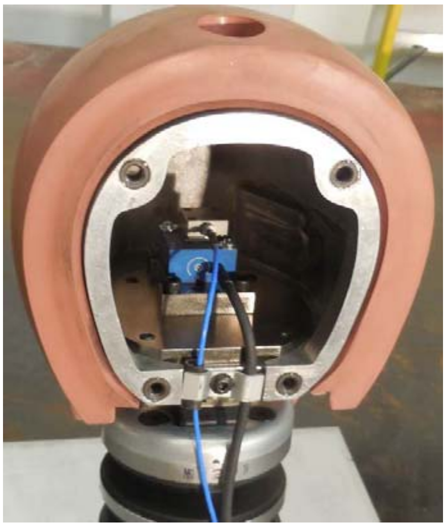

Fig. 5. Triaxial cluster of linear accelerometers shown inside the headform.


Fig. 6. High-speed camera set-up (NAC GX-8) used for both shock tube and free-field blast testing.

### *Matching Free-Field Explosive and Shock Tube Static Blast Parameters*

Static blast parameters (peak incident overpressure, peak incident impulse) were measured for the shock tube configuration, without the headform, to avoid any undue distortion of the pressure field. The tube driver was pressurised with ultra dry compressed air until the diaphragm (three layers of Mylar) ruptured, at approximately 530 kPa. For this baseline test, a piezo-electric pressure transducer was located 0.15 m away from the muzzle, along the longitudinal axis of the tube. The shock tube was fired and overpressure data were recorded.

The Blast Effects BEC computer software [10], based on the Kingery-Bulmash equations [11], was used in an iterative fashion to estimate the mass of explosive and the range required to replicate the pressure and impulse measured outside the shock tube. The explosive was modelled as a hemisphere, placed on the ground, with a TNT equivalency of 1.3 for both pressure and impulse.

A first arena test was performed using the mass of explosive and range calculated with the BEC. The static overpressure was measured using the same pencil gauge used in the shock tube test. After the test, the BEC was used (iteratively) to determine the actual TNT equivalency of the C4 explosive used, based on the resulting overpressure trace and associated impulse. Using the revised TNT equivalencies (1.3 for overpressure and 0.8 for impulse), the required mass and range were recalculated. A single iteration of this procedure resulted in a blast configuration with peak static overpressure and peak blast impulse reasonably matching the values measured for shock tube cases. The resulting blast parameters are summarised in Table I. An explosive charge mass of 0.080 kg is representative of typical anti-personnel blast mines, which range from 28 g to 240 g of TNT. The resulting overpressure and blast impulse traces are illustrated in Fig. 7 and Fig. 8, respectively.

TABLE I
MEASURED STATIC BLAST PARAMETERS

| Configuration | Peak Overpressure (kPa) | Peak Blast Impulse (kPa-ms) |
|---|---|---|
| Shock Tube – Baseline Test (Driver at 515 kPa, 3 Mylar) | 112 | 31.2 |
| Free-Field Blast – Test 1 (0.080 kg C4, 1.43 m standoff) | 129 | 34.7 |
| Free-Field Blast – Test 2 (0.080 kg C4, 1.43 m standoff) | 102 | 32.5 |
| Free-Field Blast – Test 3 (0.080 kg C4, 1.43 m standoff) | 92 | 30.4 |
| Free-Field Blast – Test 4 (0.080 kg C4, 1.43 m standoff) | 128 | 32.8 |

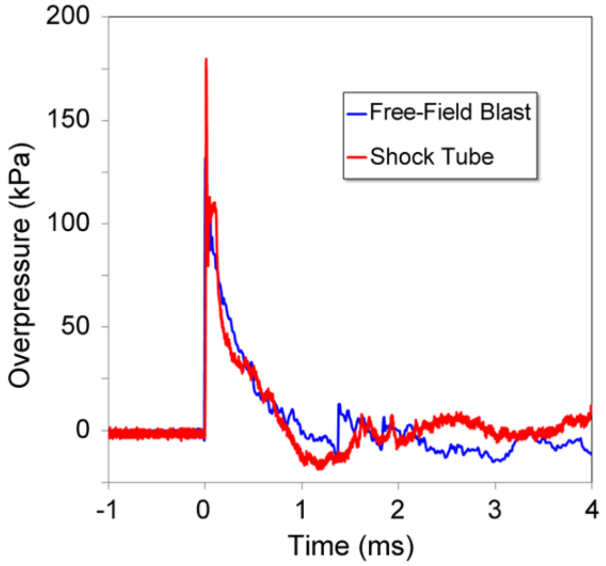


Fig. 7. Static overpressure traces for shock tube (baseline test) and free-field blast testing (Test 2).

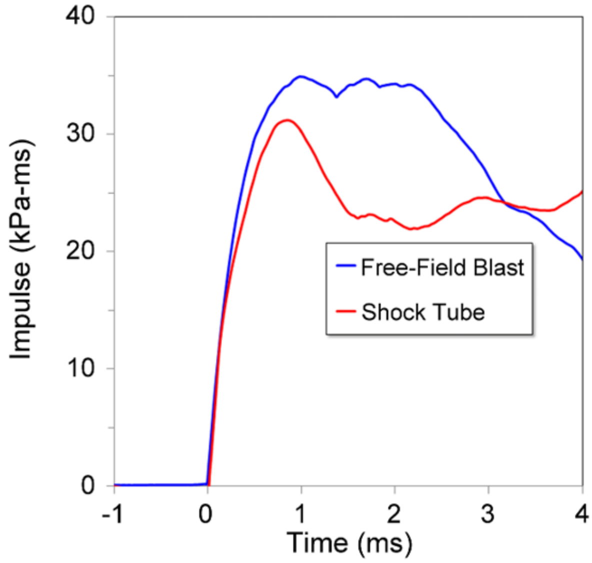


Fig. 8. Blast impulse traces (integration of traces from Fig. 7) for shock tube and free-field blast testing.

## III. RESULTS

***Head Acceleration Measurements***

For the purpose of this study, three shock tube trials (all in the same configuration) and four free-field blast trials (also all in the same configuration) were conducted. Figures 9 and 10 provide the Hybrid III head acceleration traces measured for the shock tube and free-field blast cases, respectively, in the global X-direction (headform antero-posterior direction). These figures show that the main portion of the acceleration signals is contained within the first two milliseconds of the traces.

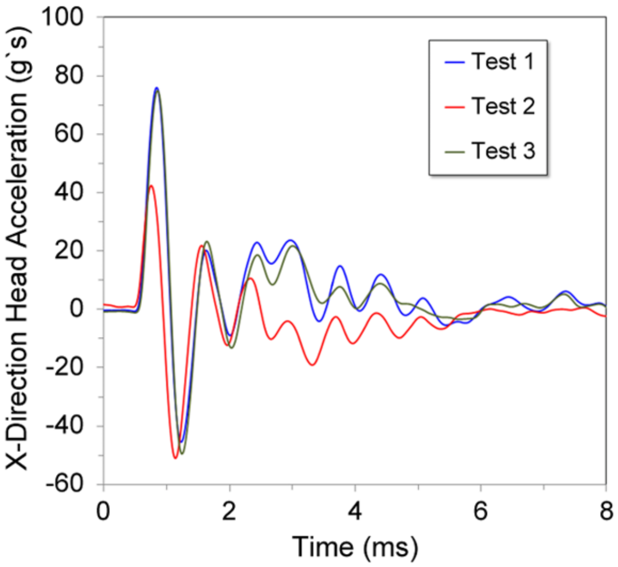


Fig. 9. Hybrid III head acceleration traces in the X-direction (antero-posterior direction) for the shock tube configuration.

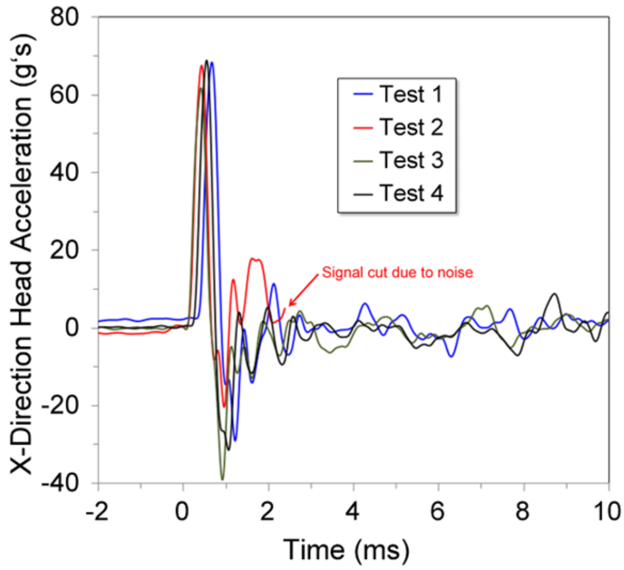


Fig. 10. Hybrid III head acceleration traces in the X-direction (antero-posterior direction) for the free-field blast configuration.

Figure 11 compiles the resultant peak head accelerations for all tests conducted. No significant differences in peak resultant accelerations were found between the shock tube and the free-field test (p=0.01). Figure 12 compares the headform X-direction acceleration histories for selected shock tube (Test 1) and free-field blast (Test 2). While there is a reasonable match in the earlier portion of the signal (up to approximately 1.5 ms), the acceleration trace remains higher afterwards. The difference between the two configurations in terms of the entirety of head inertial signal history is further evidenced by the X-direction velocity as obtained from integrating the acceleration signals (Fig. 13). Therefore, despite the similar blast exposure in terms of static overpressure and blast impulse highlighted in Fig. 7 and Fig. 8, the shock tube and free-field blast experiments induced a substantially different headform velocity response when considering the entire event duration.

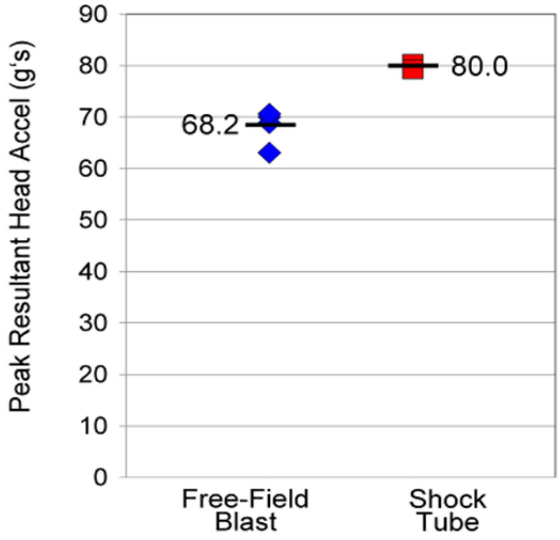


Fig. 11. Hybrid III head acceleration traces in the X-direction (antero-posterior direction) for the free-field blast configuration.

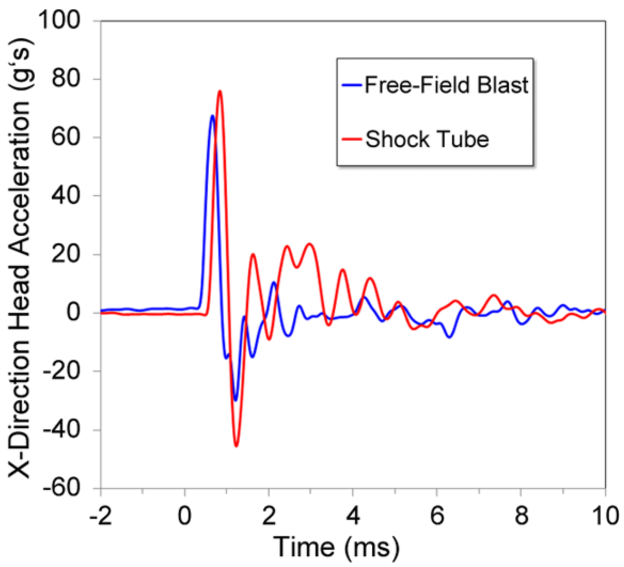


Fig. 12. Comparison of Hybrid III head acceleration traces in the X-direction (antero-posterior) for the shock tube configuration (Test 1) and the free-field blast configuration (Test 2).

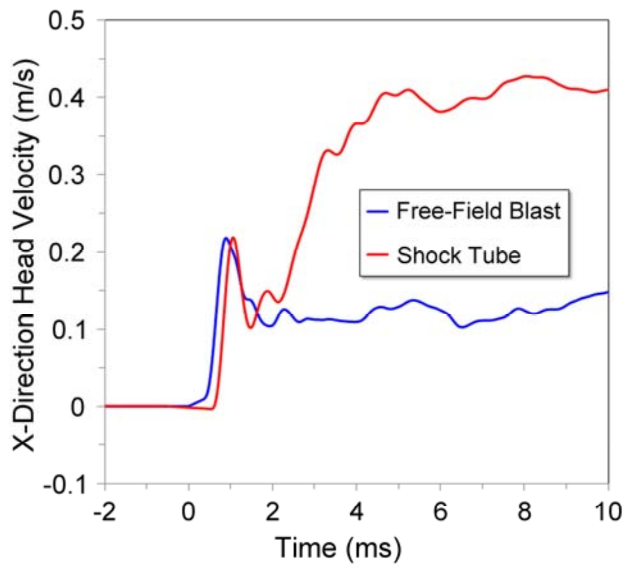


Fig. 13. Comparison of Hybrid III head velocity traces in the X-direction (antero-posterior) for the shock tube configuration (Test 1) and the free-field blast configuration (Test 2).

### *Head Kinematics from High-Speed Camera*

There was no discernible head movement for free-field blast scenarios, as evidenced by Fig. 14; this, however, was not the case for the shock tube tests (Fig. 15) which exhibits both a head displacement and head rotation. The total head excursion path and the displacements-time history for the first 100 ms are shown in Fig. 16 and Fig. 17, respectively. The peak displacements (Fig. 17) occurred at about *t*=60 ms, which is significantly later than the passage of the main phase of the shock wave (2 ms), as depicted in Fig. 7. Head motion data are expressed in the global frame of reference and in the plan of the headform sagittal plane.

Fig. 14. Still images from the high-speed camera showing the headform at rest (0 ms), 30 ms and 60 ms, for a free-field blast case (Test 2).

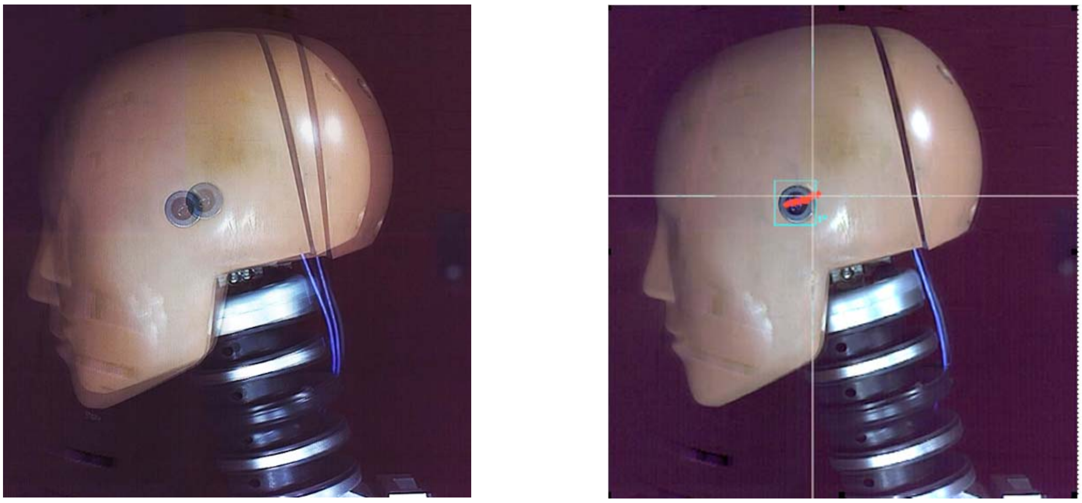

Fig. 15. Superimposed still images of the start and maximum excursion of the head (left) for the shock tube configuration (Test 1). Centre of gravity travel path is plotted on an image (right) of the headform in the start position for the same test.

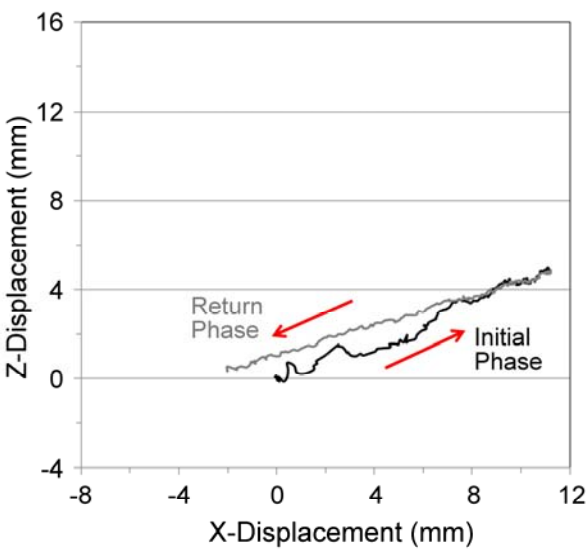


Fig. 16. Head excursion from the high-speed camera and analysed with the ProAnalyst motion tracking system package (Shock Tube – Test 1).

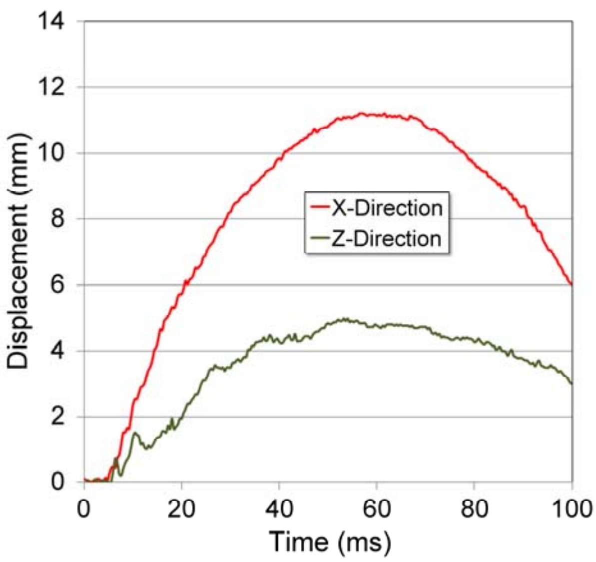


Fig. 17. Head displacements with respect to time for both the X (antero-posterior) and Z (bottom to top) directions from the high-speed camera, and analysed with the ProAnalyst motion tracking system package (Shock Tube – Test 1).

A direct comparison between the accelerometer data and the high-speed video data was not possible, since the parameters measured are different (acceleration vs. displacement). However, in both cases, transformations were made to express both sets of data in terms of head velocities. In the accelerometer data case, the X-direction acceleration time history was integrated. For the shock tube case, the X-direction displacement data was first smoothed using a 16-point moving average and then differentiated to obtain velocity. The two resulting velocity curves are shown in Fig. 19. It can be seen that the high-speed video data appropriately captured both the acceleration and the deceleration phases, as visible from the close match between the two velocity curves, which provides a rationale for the use of high-speed camera data.

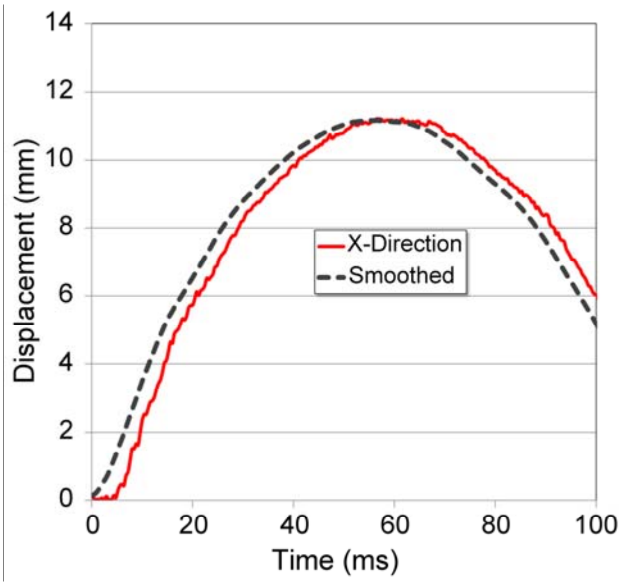


Fig. 18. Smoothing of the X-direction head excursion data captured by the high-speed camera using a 16-point moving average, for a shock tube test (Test 1).

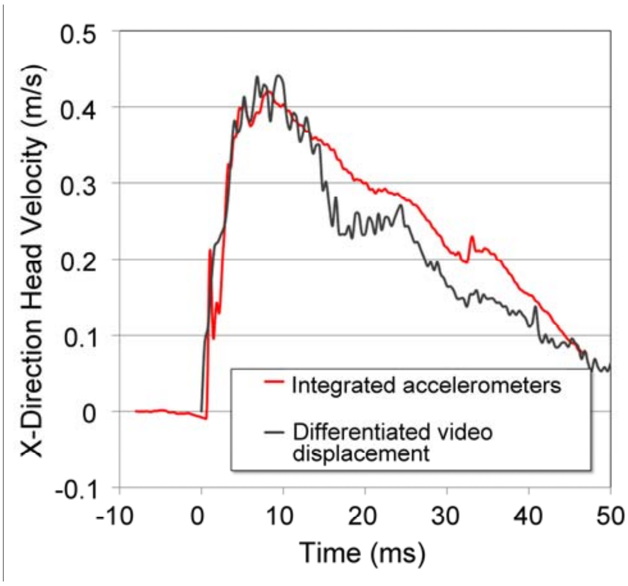


Fig. 19. Comparison of headform X-velocity traces (Shock Tube – Test 1) obtained by integrating the accelerometer signal, and by differentiating the curve fit from Fig. 18 for the high-speed video displacement data.

## IV. DISCUSSION

Our data demonstrated that the initial portion (first two milliseconds) of the head kinematic response under the shock tube configuration (0.15 m away from the muzzle) was similar to the free-field explosive blast loading configuration (Fig. 12 and Fig. 13). The noted head kinematic response similarity (in x-direction acceleration traces and peak head accelerations) is consistent with the static peak overpressure and the peak impulse similarities within the corresponding first two milliseconds of the signals at most (Fig. 7 and Fig. 8). However, beyond this time window, large deviations in head displacement were noted between the shock tube and free-field blast configurations. These deviations were evidenced by high-speed video analysis and by integrating acceleration data over a longer portion of the signals (Fig. 13). The time window during which the shock tube static pressure data closely matches the equivalent free-field data is expected to vary depending on the blast strength.

The fact that the head kinematics response differed in the two configurations, despite the static overpressure and peak impulse being approximately matched, suggests that other blast parameters come into play. In this regard, Josey *et al.* [12], who had simulated free-field pressure-time histories using the DRDC Advanced Blast Simulator (ABS), suggested that the dynamic pressure must also be matched in the shock tube testing to generate a pressure field representative of a free-field blast.

However, the Josey *et al.* study [12] focused only on field pressure measurements and did not consider the effects of the loading on a headform. The current study was aimed at addressing this gap by introducing a Hybrid III headform and neck assembly as a test surrogate, so that parameters of relevance to helmet performance testing could be considered. The head responses measured in the current work did confirm that matching the peak static overpressure and peak impulse was necessary, but not sufficient to appropriately model free-field explosive blast loading, which confirms the observations of Josey *et al*. [12].

Shock tubes may also be used towards the investigation of blast-induced brain injury mechanisms employing animal models. Our study showed that even if the peak static pressure and impulse are representative of free-field blast, the head kinematics occurring later during the event were not. This late kinematics behaviour is expected to introduce an artificial secondary inertial loading at the neck level (not measured in the present study). If, in the course of its movement, the head collides with rigid components of the test jig, the compounding effect on the brain cannot be delineated from the more representative initial response of the head. This issue has been demonstrated by Needham et al. [6] in tests whereby the head of a rat held near the shock tube exit and perpendicular to the flow, made a violent focal impact against the rim of the canister that was holding the rat in place.

Furthermore, on the basis of the data presented in this work, it can be hypothesized that locating a headform outside of a shock tube is unlikely to be appropriate for injury investigations, unless it could be demonstrated that only the initial loading (first few milliseconds) is of relevance towards injury.

The Hybrid III headform used in the current study is not fully biofidelic. For instance, it does not contain any internal head features (e.g. materials representative of brain tissues), and its neck has not been validated for blast exposure. Yet, given its representative mass, mass balance and overall size, the Hybrid III neck and head assembly proved useful to illustrate the importance of matching the kinematic head loading towards validation of shock tube test apparatuses aimed at evaluating helmet performance. The authors believe that a shock tube apparatus that generates Hybrid III headform loading in line with free-field explosive blast loading will also generate representative blast loading for more advanced head surrogates and biological models.

While the ultimate objective of this work is to develop a test method for the blast attenuation performance of helmets, only an unprotected Hybrid III headform was tested. The authors believe that helmet testing can only be relevant if pressure fields sufficiently representative of free-field explosive blast can be replicated by shock tube apparatuses.

## V. CONCLUSIONS

The present study has demonstrated that while the pressure field outside of a shock tube can be tuned to replicate the static peak overpressure and peak impulse of a free-field explosive blast, the kinematic response of a Hybrid III headform in that flow field did not correspond to the free-field blast case, especially in terms of head displacement and head velocity, beyond the first few milliseconds. It was therefore concluded that matching the static pressure measurements (peak pressure, peak impulse) is necessary, but not sufficient for a shock tube to appropriately replicate the pressure fields generated by a high explosive charge detonated in the free-field. Accounting for the dynamic pressure may be more appropriate.

## VI. ACKNOWLEDGEMENTS

The authors wish to thank Mr Rick Guilbault (CanmetCERL) for his assistance with setting up the tests and conducting the high-speed video analysis, as well as Mr Doug Bueley (Med-Eng) for his assistance with the instrumentation of the Hybrid III headform.

## VII. REFERENCES

[1] ASTM F-1446, Standard Test Methods for Equipment and Procedures Used in Evaluating the Performance Characteristics of Protective Headgear, ASTM, Pennsylvania 19428-2959.

[2] Riot Helmets and Faceshield Protection, Canadian Standards Association Z611-02, August 2002.

[3] "FRONTIERS IN HEAD AND NECK TRAUMA, Clinical and Biomechanical", N. Yoganandan et al. (Eds.), IOS Press, OHMSHA (c) 1998 ()

[4] Carneal, C., *et al*. (2016) Development of a Laboratory Shock Tube System for Helmet Blast Overpressure Performance Assessment. *Proceedings from the Personal Armour Systems Symposium (PASS)*, September 2016, Amsterdam, Netherlands.

[5] Yu, A., *et al*. (2014) In vs. Out: Controversies in Shock Tube Blast Experiments. *Proceedings from the 2014 Personal Armour Systems Symposium (PASS)*, September 2014, Cambridge, UK.

[6] Needham, C. E., Ritzel, D., Rule, G. T, Wiri, S. and Young L. (2015) Blast testing issues and TBI: experimental models that lead to wrong conclusions. *Frontiers in Eurology*, **6**(72): pp.1–10.

[7] Bass, C. R., *et al*. (2005) A Methodology for Assessing Blast Protection in Explosive Ordnance Disposal Bomb Suits. *International Journal of Occupational Safety and Ergonomics*, **11**(4): pp.347–36.

[8] Haladuick, T., et al. (2012) Head Kinematics Resulting from Simulated Blast Loading Scenarios. *Personal Armour Systems Symposium (PASS)*, 2012, Nuremberg, Germany.

[9] Instrumentation for Impact Test, Part 1, Electronic Instrumentation, SAE J211-1, 1995.

[10] Department of Defense Explosives Safety Board (2008) Blast Effects Computer, version 6.3.1.

[11] Kingery, C. N. and Bulmash, G. (1984) Airblast parameters from TNT spherical air burst and hemispherical surface burst, ARBRL-TR-02555. Ballistic Research Laboratory, Aberdeen Proving Ground, MD, USA.

[12] Josey, T., Sawyer, T. W., Ritzel, D., Donahue, L. (2016) High Fidelity Simulation of Free Field Blast Loading: The Importance of Dynamic Pressure. *Proceedings from the Personal Armour Systems Symposium (PASS)*, September 2016, Amsterdam, Netherlands.